Journal of Medicinal Chemistry

Article

pubs.acs.org/jmc

Synthesis, Anticancer Activities, and Cellular Uptake Studies of Lipophilic Derivatives of Doxorubicin Succinate

Bhupender S. Chhikara, Deendayal Mandal, and Keykavous Parang*

Department of Biomedical and Pharmaceutical Sciences, College of Pharmacy, University of Rhode Island, 41 Lower College Road, Kingston, Rhode Island 02881, United States

Supporting Information

ABSTRACT: A number of lipophilic 14-substituted derivatives of doxorubicin were synthesized through conjugation of doxorubicin-14-hemisuccinate with different fatty amines or tetradecanol to enhance the lipophilicity, cellular uptake, and cellular retention for sustained anticancer activity. The conjugates inhibited the cell proliferation of human leukemia (CCRF-CEM, 69−76%), colon adenocarcinoma (HT-29, 60−77%), and breast adenocarcinoma (MDA-MB-361, 66−71%) cells at a concentration of 1 μM after 96−120 h of incubation. The *N*-tetradecylamido derivative of doxorubicin 14-succinate (**10**) exhibited consistently comparable antiproliferative activity to doxorubicin in a time-dependent manner (IC_{50} = 77 nM in CCRF-CEM cells). Flow cytometry analysis showed a 3-fold more cellular uptake of **10** than doxorubicin in SK-OV-3 cells. Confocal microscopy revealed that the conjugate was distributed in cytoplasmic and perinuclear areas during the first 1 h of incubation and slowly relocalized in the nucleus after 24 h. The cellular hydrolysis study showed that 98% of compound **10** was hydrolyzed intracellularly within 48 h and released doxorubicin.

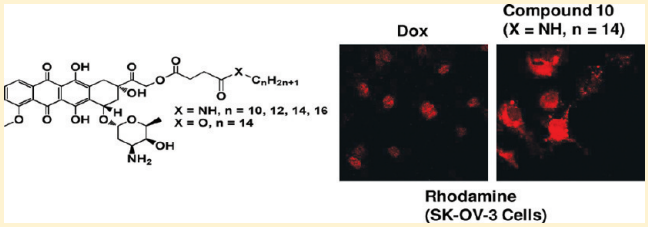

INTRODUCTION

The development of anticancer drugs with a high therapeutic index is a subject of considerable interest in cancer chemotherapy. The biological activity and toxicity of low molecular weight anticancer drugs depend on their physicochemical properties[1−3] that contribute to the pharmacokinetics, biodistribution, cellular retention, and bioavailability in the target tissue or organ. The activity and toxicity associated with an anticancer drug can be modulated by altering the physicochemical properties, such as lipophilicity, cellular uptake, and prolonged activity, through chemical conjugation.

Doxorubicin (Dox, Scheme 1) is an anthracycline antibiotic commonly used as an anticancer agent in the treatment of leukemia, breast carcinoma, and other solid tumors.[4] Although Dox is also used for treating other tumors like ovarian carcinoma, liver cancer, and stomach cancer, it is not the first choice in the clinic for these cancers due to the emergence of drug resistance.[5] Dox does not show high antiproliferative activity against ovarian carcinoma cell line SK-OV-3, showing an IC_{50} value of 5 μM following 48 h of incubation.[6] The highly hydrophilic nature, high volume of distribution, and short half-life of Dox[7−9] cause the rapid distribution, excretion, and low bioavailability of the drug. Furthermore, Dox is actively extruded from cancer cells overexpressing P-glycoprotein (PgP).[10] Thus, high cumulative doses of Dox are required in cancer chemotherapy to achieve sufficient therapeutic effect. However, higher doses lead to dose-dependent side effects, such as cumulative cardiotoxicity, nephrotoxicity, and extravasation, which compromises its clinical applications.[11,12]

Moreover, intracellular Dox accumulation is a complex process, which includes cellular uptake, retention and relocalization, and efflux from the cell. At any given time, the net uptake (accumulation) of the drug in cells is the difference between the quantity of drug uptake and the efflux. Thus, it is required to design the next generation of Dox derivatives to overcome the drug resistance, to improve the retention in the cell, and to enhance the sustained therapeutic effect.

A number of approaches have been examined to improve the efficacy or delivery of Dox, including using proteins,[13] nanoparticles (e.g., fullerenol, gold nanoparticles, and nanospheres),[14−17] liposomes,[18−22] and peptides,[23,24] dendrimers,[25] or hydrogels.[26]

Alternatively, a prodrug strategy by chemical modification or conjugation with a parent drug[27,28] has been extensively used in the delivery of drugs including Dox. A lipophilic derivative obtained by conjugation of docosahexanoic acid with Dox displayed a significantly higher anticancer activity than free Dox in vivo following intraperitoneal injection in L1210 leukemia ascites model.[29] The 6-maleimidocaproyl)hydrazone derivative of Dox, an albumin-binding derivative of Dox (formerly DOXO-EMCH, INN-206), is currently under phase II clinical trial.[30]

A systematic study of fatty acyl conjugates of Dox is still in a very nascent stage and remains relatively unexplored. We recently reported different fatty acyl amide derivatives of Dox with substitution at the 4′-amine group of the sugar segment.[31] DNA intercalation by Dox leads to inhibiting the ability of

Received: August 18, 2011
Published: January 25, 2012

Scheme 1. Chemical Synthesis of Fatty Acyl-Dox Conjugates (8−13)[a]

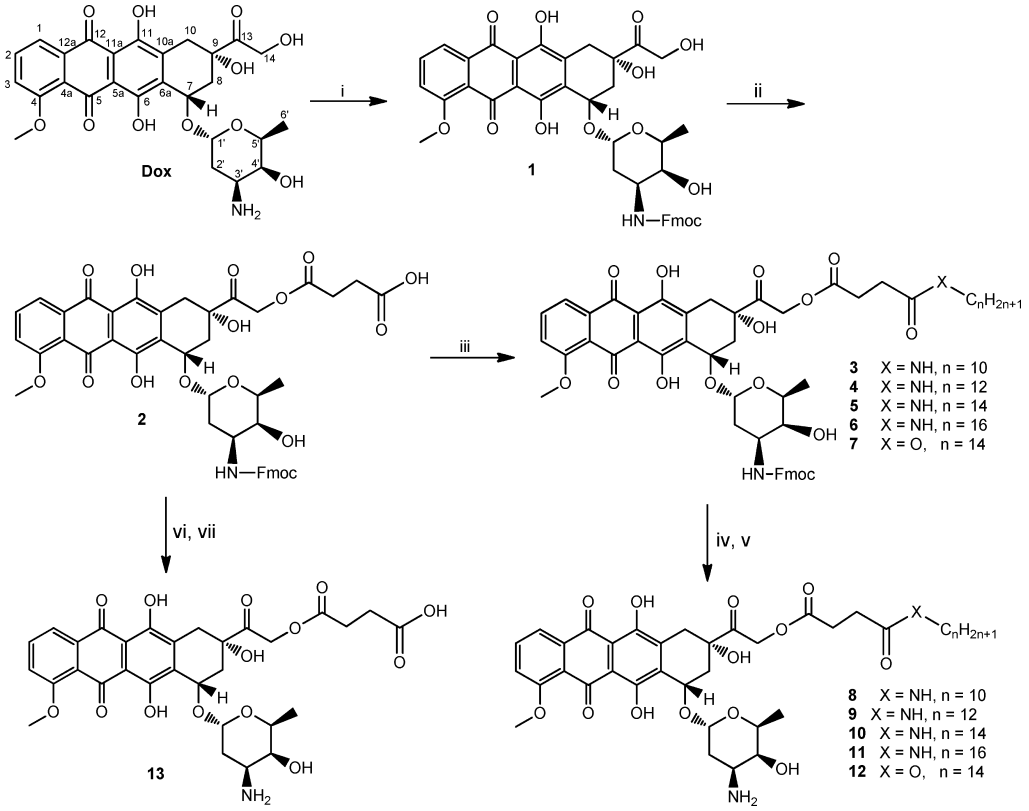

[a]Reagent and conditions: (i) Fmoc-OSu, DIPEA, DCM. (ii) Succinic anhydride, DIPEA, DMF. (iii) C_nH_{2n+1}−X, X = NH_2 or OH (n = 10, 12, 14, or 16), HBTU, DIPEA, DMF. (iv) Piperidine/DMF (5%), RT, 10 min. (v) HOAc, TFA. (vi) Piperidine/DMF (8%), RT, 10 min. (vii) TFA.

topoisomerase II (Topo II) to reseal the DNA double helix strands during the replication and thereby stops the cell reproduction.[32,33] Substitution at the sugar moiety led to reduced antiproliferation activity of the drug. A free carbohydrate portion of the drug is required for effective intercalation with the flanking base pairs in DNA. Furthermore, the planar aromatic portion of Dox intercalates between two base pairs of the DNA helix and cannot be modified through conjugation. Thus, further studies are required to design other fatty acyl derivatives of Dox and to establish their structure−activity relationships.

Herein, we report the synthesis of fatty acyl derivatives of Dox (Scheme 1) through conjugation with different lipophilic chains at 14-hydroxyl group and assessment of their in vitro anticancer activities in different cancer cell lines, lipophilicity, stability, and cellular uptake and retention. The conjugates were designed to enhance the lipophilic nature and cellular uptake, to prolong biological activity, and to reduce the intrinsic cellular efflux of Dox.

RESULTS AND DISCUSSION

Chemistry. Scheme 1 depicts the synthesis of fatty acyl derivatives of 14-Dox succinate. Amide and ester bonds were used to attach the fatty acids to Dox through an ester succinate linker at position 14. The protection of primary amine in Dox with a Fmoc group was accomplished by the reaction of Dox with *N*-(9-fluorenylmethoxycarbonyloxy)succinimide (Fmoc-OSu) in the presence of *N*,*N*-diisopropylethylamine (DIPEA) to afford Fmoc-doxorubicin (**1**) as described previously.[24]

N-Fmoc-doxorubicin (**1**) was reacted with succinic anhydride in the presence of DIPEA to yield the intermediate *N*-Fmoc-doxorubicin-14-hemisuccinate (**2**) according to the previously reported procedure.[24] Monosubstituted fatty acyl amide-Dox succinate conjugates (**8**−**11**) were obtained by amidation reaction of **2** with fatty amines [i.e., $CH_3(CH_2)_zNH_2$ (z = 9−15)] (1 equiv) in the presence of 1,1,3,3-tetramethyluronium hexafluorophosphate (HBTU) and DIPEA followed by deprotection with piperidine (Scheme 1). Similarly, acylation reaction of **2** with tetradecanol afforded the conjugate ester derivative **12**. Deprotection of Fmoc group in **2** afforded Dox hemisuccinate (**13**). The final products were purified with silica gel flash chromatography using dichloromethane and methanol (0−20%) as eluents. Further purification was carried out by reverse phase HPLC using water and acetonitrile as gradient solvents. The structures of the synthesized derivatives were confirmed by using infrared spectroscopy, nuclear magnetic resonance (NMR) spectroscopy (^{1}H, ^{13}C, or DEPT), and high-resolution time-of-flight electrospray mass spectrometry. The purity of the final products (≥95%) was confirmed by reverse phase analytical HPLC using two different gradient systems of water (0.1% TFA) and acetonitrile (0.1% TFA) (method A1, 12 min run; and method A2, 20 min run).

While the Dox and Dox-hemisuccinate (**13**) were highly soluble in aqueous medium, most of the fatty acyl Dox derivatives were soluble in organic solvents (e.g., CH_2Cl_2, $CHCl_3$, CH_3OH, and DMSO). Compound **8** with a 10-carbon chain length was soluble in water as well as in organic solvents. All of the derivatives had a dark reddish color.

dx.doi.org/10.1021/jm201653u | J. Med. Chem. 2012, 55, 1500−1510

Lipophilicity of many compounds is usually correlated with the membrane permeability and/or biological activity in quantitative structure−activity relationship studies. Partition coefficients (Log *P*) of **8**−**13** were determined using a biphasic *n*-octanol/water shake flask method. The concentration of the compounds was measured in both phases using UV−visible spectroscopy. The Log *P* values of Dox derivatives increased with the gradual increase in chain length of the attached fatty acyl groups. Partition coefficients (Log *P*, octanol/water) values varied from 0.2 to 1.08 for the synthesized derivatives versus Dox (Log *P* = −0.5).

Figure 1 demonstrates the distribution of the compound in *n*-octanol for more lipophilic compounds and in water for hydrophilic compounds. The higher retention time in reverse phase analytical HPLC further confirmed the higher lipophilicity for compounds with a longer chain length (see the Supporting Information).

Biological Activity. The effect of compounds on the cell proliferation of cancer cells was evaluated in vitro in human leukemia (CCRF-CEM), breast adenocarcinoma (MDA-MB-468, MDA-MB-361), ovarian adenocarcinoma (SK-OV-3), and colon adenocarcinoma (HT-29) cell lines up to 120 h at a concentration of 1 μM (Figure 2). The cell proliferation assay was carried out using CellTiter 96 aqueous one solution cell proliferation assay kit (Promega, United States).

In general, the effects of compounds on cell proliferation of cancer cells found to be time-dependent with more growth inhibitory effects were observed after 96 h. These data indicate that the lipophilic compounds may have a prolonged effect possibly due to the sustained intracellular hydrolysis to Dox and nuclear relocalization for effective intercalation. Furthermore, free succinate analogue **13** showed comparable activity to Dox in all cell lines. These data suggest that a relatively labile and cleavable succinate ester bond at position 14 could allow Dox release.

The synthesized conjugates inhibited the cell proliferation of CCRF-CEM (69−76%), HT-29 (60−77%), MDA-MB-468 (49−63%), MDA-MB-361 (66−71%), and SK-OV-3 (54−62%) cells at a concentration of 1 μM after 96−120 h of incubation. The antiproliferation activity of compounds **8**−**13** was relatively cell-specific in the order CCRF-CEM and HT-29 > MDA-MB-468, MDA-MB-361 > SK-OV-3 for most of the compounds. This is consistent with earlier results exhibiting low antiproliferative activity of Dox against ovarian cancer with an IC_{50} value of 5 μM.[6] All of the compounds exhibited consistently comparable antiproliferative activity with IC_{50} values of 75−77 nM against CCRF-CEM cancer cells when compared to Dox with an IC_{50} value of 45 nM after 96 h of incubation. Compound **10** inhibited the cell proliferation of MDA-MB-468 cells by 70.2% after 120 h of incubation comparable to that of Dox (69.1%). Myristoyl amide derivative **10** exhibited slightly more antiproliferative activity in all cell lines when compared with that of the corresponding myristoyl ester derivative **12**. These data indicate that the antiproliferative activity of Dox was not compromised with conjugation of Dox at position 14 with succinyl or lipophilic fatty chains, and a sustained effect can be generated through conjugation.

Cellular Uptake. Dox is colored and has significant fluorescence in the visible region. Thus, the optical properties of Dox provide opportunities to track and compare Dox and fatty acyl conjugates by using fluorescence-based techniques. In vitro antiproliferative studies suggested that compound **10** was optimal among fatty acyl-Dox conjugates. Thus, the cellular uptake of Dox and Dox derivative **10** was examined in SK-OV-3 cells by fluorescence-activated cell sorter (FACS) analysis (Figure 3) showing a 3-fold more cellular uptake of **10** when compared to Dox alone in Dox-resistant SK-OV-3 cells. These data suggest that the attachment of *N*-tetradecylamine to 14-Dox succinate in **10** enhances the cellular uptake.

The subcellular localization of free Dox and **10** was investigated after short-term exposure in SK-OV-3 cells. Figure 4 shows the confocal microscopy images of SK-OV-3 cells after 1 h of incubation with compound **10**. A noncytotoxic concentration of 5 μM was chosen to ensure Dox fluorescence detection by confocal microscopy. As shown, free Dox and Dox derivative **10** did not exhibit a similar pattern of cellular

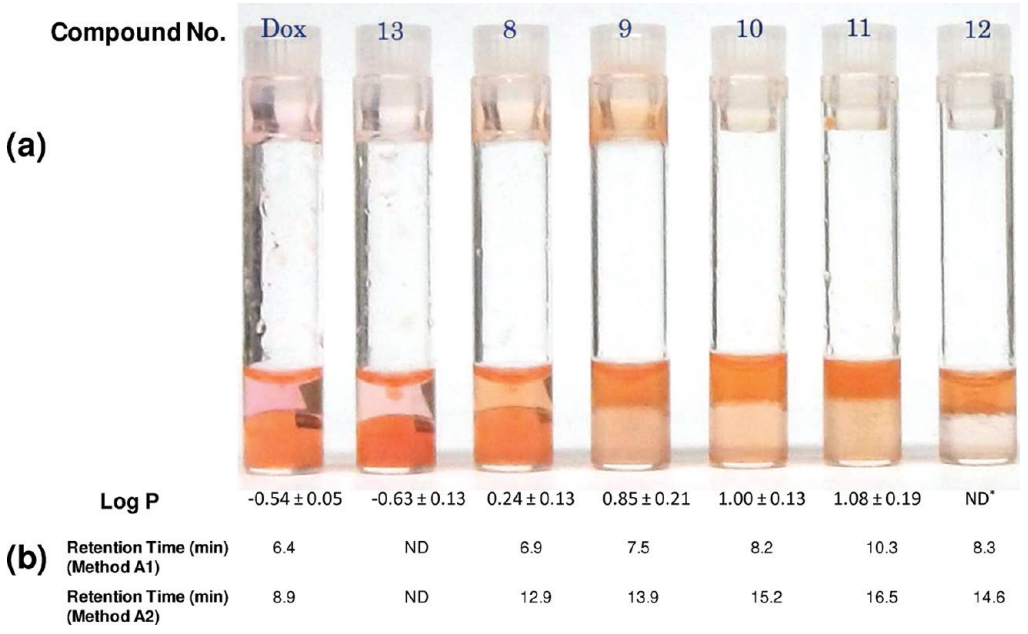

Figure 1. (a) Biphasic (octanol/water) distribution of Dox derivatives (**8**−**13**) (ND*, not determined). (b) Analytical HPLC retention time using a gradient system of water (0.1% TFA) and acetonitrile (0.1% TFA): method A1, 12 min run; and method A2, 20 min run (Supporting Information).

dx.doi.org/10.1021/jm201653u | *J. Med. Chem.* 2012, 55, 1500−1510

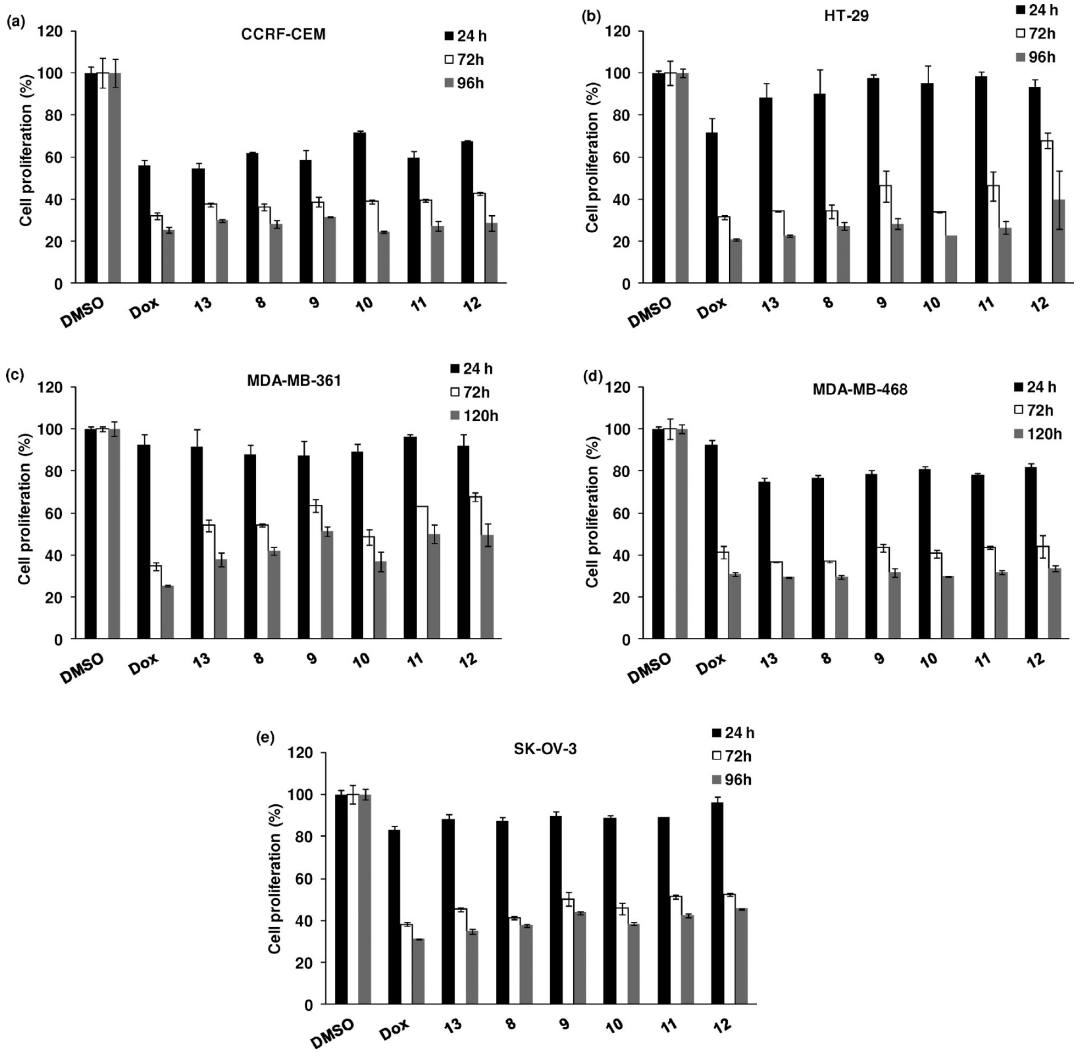

Figure 2. Antiproliferative activity of Dox and **8**–**13** (1 μM) in (a) CCRF-CEM, (b) HT-29, (c) MDA-MB-361, (d) MDA-MB-468, and (e) SK-OV-3 cells after 24, 72, 96, or 120 h. The results are shown as the percentage of the control that has no compound (set at 100%). All of the experiments were performed in triplicate.

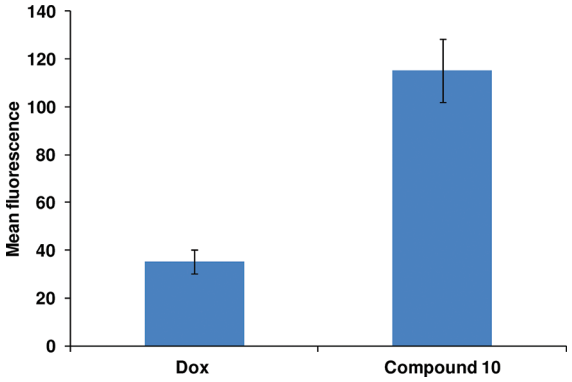

Figure 3. Cellular uptake of Dox (5 μM) and compound **10** (5 μM) in SK-OV-3 cells.

distribution. After 1 h of incubation, free Dox localized mainly in the nucleus. In contrast, compound **10** was distributed mainly in the cytoplasm. The conjugate was found to be readily taken by the cells. The results indicate that the cells accumulate significant amounts of Dox derivative **10** over Dox alone.

Obviously, conjugation of Dox to fatty acids prevented the accumulation of Dox into the nuclei of the cells. Moreover, the greater apparent fluorescent intensity observed in case of **10** indicates that fatty acid conjugation allows a greater accumulation of the drug in cells. The resided conjugate in the cytoplasm could release free Dox gradually or could reach slowly into the nucleus and release Dox. In both cases, free Dox eventually causes DNA intercalation and inhibition of Topo II. These results are consistent with the sustained effect of compound **10**.

SK-OV-3 cells were exposed to **10** and free Dox for 1 h and further incubated in drug-free medium for 24 h to investigate the drug efflux. Dox fluorescence in cells treated with free Dox disappeared almost entirely in contrast to a significant residual fluorescence in cells treated with **10** (Figure 5) that showed enhanced nuclear localization. This result indicates that compound **10** was retained in cells much longer than that of free Dox and then was relocalized slowly into the nucleus.

The cytotoxic effects of Dox and compound **10** on SK-OV-3 cell line were investigated using the MTT assay. The cells were incubated with Dox or compound **10** (up to a maximum of 10 μM) for 2 h and then with compound-free medium for 72 h. The data showed a higher cytotoxicity of compound **10** than that of Dox at a concentration of 100 nm and above after 72 h of incubation (Figure 6). Dox (10 μM) showed 51.5 $\pm$ 2.5% cytotoxicity after 72 h of incubation. In contrast, the

dx.doi.org/10.1021/jm201653u | J. Med. Chem. 2012, 55, 1500–1510

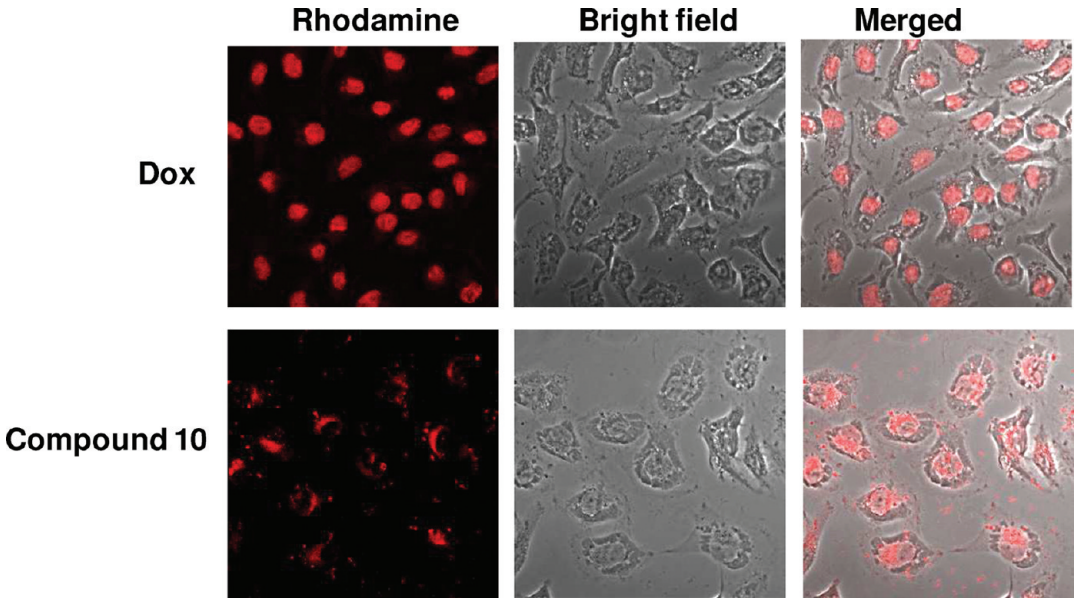

Figure 4. Confocal microscopy images of Dox and **10** (5 μM) uptake in SK-OV-03 cells after 1 h. Red represents the fluorescence of Dox.

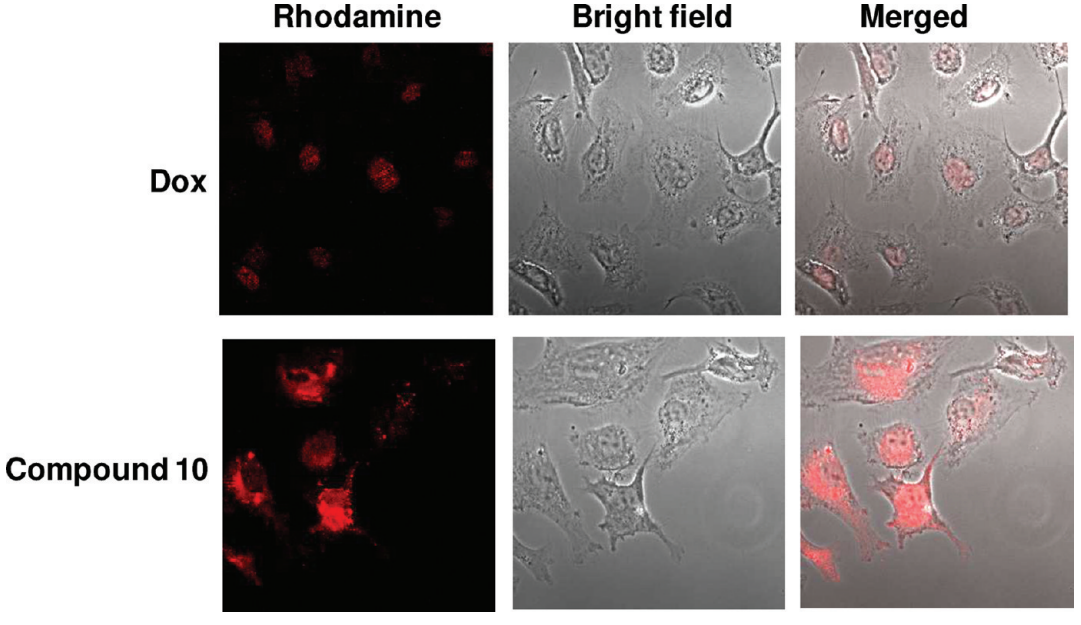

Figure 5. Confocal microscopy images of Dox and **10** (5 μM) uptake in SK-OV-03 cells. SK-OV-3 cells were treated with drug for 1 h. The compound was removed, and the cells were incubated with complete media for 24 h. Red represents the fluorescence of Dox.

cytotoxicity increased to 67.1 ± 0.8% when cells were incubated with compound **10** for 1 h and then incubated with drug-free medium. At a concentration of 5−10 μM, compound **10** exhibited approximately 1.4-fold higher cytotoxicity than Dox. The data suggest a sustained cytotoxic effect of compound **10** after 72 h. One possible explanation for this improved efficacy in cytotoxicity observed for **10** versus Dox against SK-OV-3 cells could be due to the presence of an efflux type phenomenon of the free drug. Although free Dox diffuses into the cells easily, it is effluxed rapidly from SK-OV-3 cells that show resistance to Dox at low concentrations. In contrast, the fatty acid derivative **10** was not pumped out from these cells and generated cytotoxicity even after 72 h in drug-free medium.

Topo II Inhibitory Activity. The activities of Dox and compound **10** were compared against Topo II to determine whether the conjugate has inherent inhibitory activity similar to that of the parent drug. Topo II catalyzes the double-stranded cleavage of DNA by isolating catenated DNA duplexes at the end of replication through the decatenation. Kinetoplast DNA (kDNA) is a DNA substrate commonly used in the in vitro decatenation assay. kDNA consists mainly of a large network of interlocked or catenated colvalently closed DNA minicircles. The release of minicircles from kDNA networks by Topo II can be easily visualized by agarose gel electrophoresis.

The Topo II enzyme assay for decatenation of kDNA in the presence of Dox and **10** was used to analyze the comparative inhibitory activity of the compounds. The catenated form of kDNA did not enter a 1% agarose gel (lanes A2, B2, and C2), while released minicircles migrated in to the gel (lanes A1, B1, and C1) (Figure 7). The kDNA (100 ng) was incubated with different

dx.doi.org/10.1021/jm201653u | J. Med. Chem. 2012, 55, 1500−1510

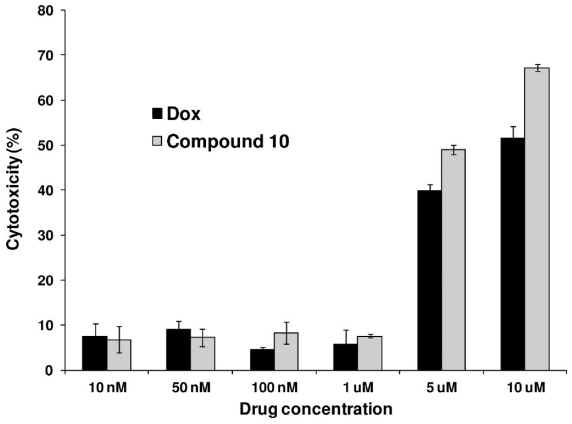

Figure 6. Cytotoxicity assay of compound **10** vs Dox in SK-OV-3 cells using MTT assay after 72 h.

concentrations of the compounds and subjected to decatenation by Topo II. Dox is an inhibitor of the DNA-decatenating enzyme Topo II. The Topo II/DNA enzyme assay revealed that compound **10** was approximately 3–4-fold less active than Dox for inhibition of Topo II enzyme activity. The decatenation of kDNA was inhibited by Dox at 5 μM (lane B4), while lipophilic compound **10** exhibited the inhibitory activity at 15–20 μM (lanes A6 and A7) as indicated by the gel images (Figure 7).

The inhibitory activities of Dox and compound **10** were compared to that of the previously reported amide derivative hexadecanoyl doxorubicin amide **14** (Dox-16),[31] a fatty acyl amide derivative of Dox with substitution at 4′-amine group of sugar segment. Compound **14** showed no inhibitory activity for Topo II under a similar condition even at the highest tested concentration (25 μM, see lanes C2–C8, Figure 7), suggesting that a free carbohydrate portion of the drug is required for effective inhibition of Topo II activity.

In a control experiment, the hydrolysis of compound **10** in the presence of the assay reaction buffer and in the absence of Topo II was monitored by HPLC, which indicated the stability of compound **10** under assay conditions (data not shown). The data indicate that the antiproliferation activity of compound **10** could be partly due to intrinsic Topo II inhibitory activity of Dox conjugate at higher concentrations.

Stability. The stability studies were performed for compound **10** with incubation with fetal bovine serum (FBS) and phosphate-buffered saline solution (PBS). The data indicated the relative stability of **10** in both systems at 37 °C with half-life values of 8.3 and 19.3 h in FBS and PBS, respectively. There was no observed precipitation or turbidity, suggesting no substantial interaction with serum proteins in FBS. The compound was more stable in PBS when compared to that of FBS. For example, 17 and 44% conversion to Dox were observed after 72 h of incubation of **10** in PBS and FBS, respectively (Figure 8).

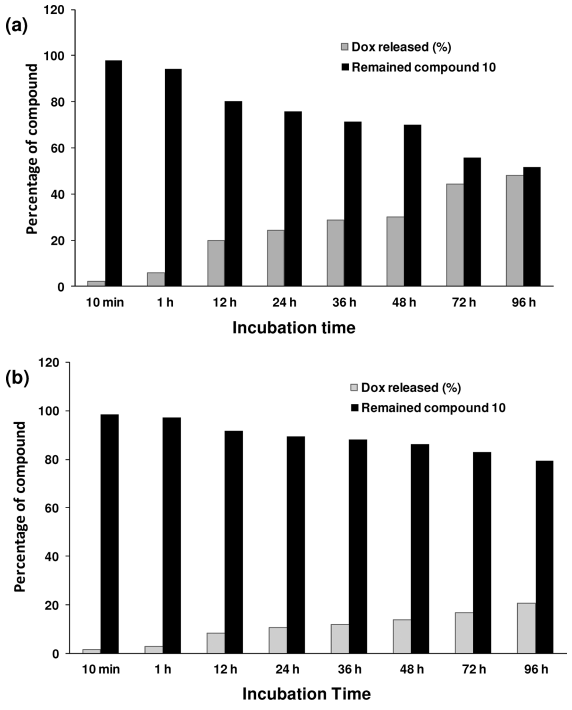

Figure 8. Stability of compound **10** after incubation with (a) FBS and (b) PBS.

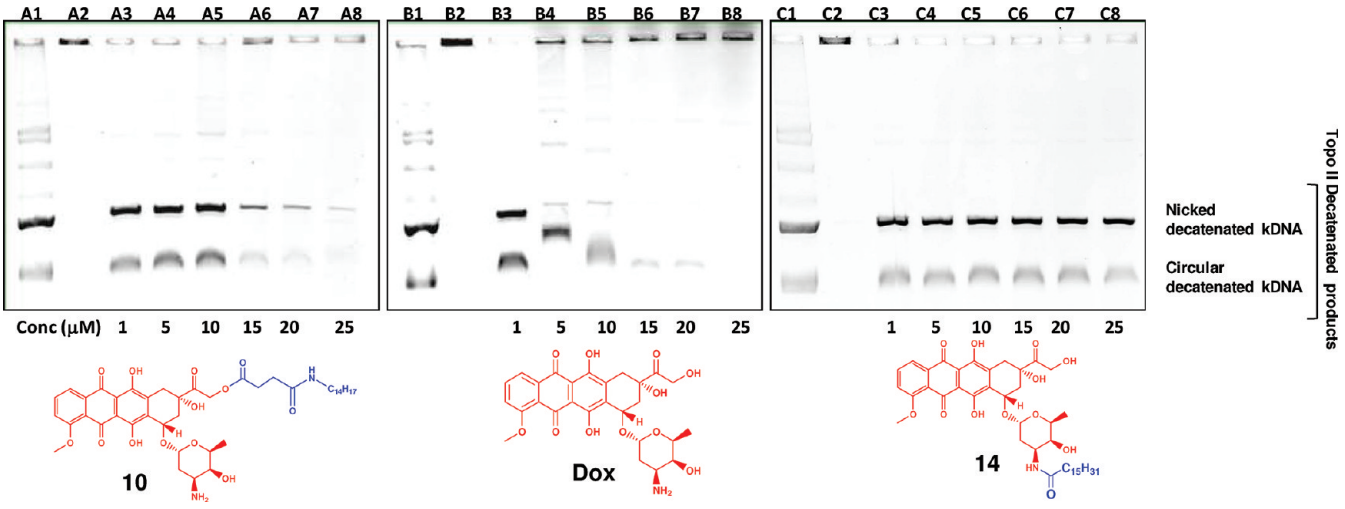

Figure 7. Topo II assay for compound **10** (left), Dox (middle), and compound **14** (right). The lines A1, B1, and C1 were decatenated DNA markers, while A2, B2, and C2 have kDNA. kDNA was incubated with compound **10** (1–25 μM, lanes A3–A8), Dox (1–25 μM, lanes B3–B8), and compound **14** (1–25 μM, lanes C3–C8) and decatenated using Topo II for 30 min at 37 °C. The decatenation was monitored by gel electrophoresis and imaged by ethidium bromide fluorescence.

dx.doi.org/10.1021/jm201653u | J. Med. Chem. 2012, 55, 1500–1510

Intracellular Hydrolysis. Intracellular hydrolysis of compound **10** was monitored in CCRF-CEM cells. The growing cells (1.37×10^7) were incubated with compound **10** (1 μM) for 4 h and then with medium only (no compound) to determine whether the conjugate undergoes intracellular hydrolysis to Dox. Drug-free medium rules out the continuous cellular uptake of the conjugate, while the compound is hydrolyzed intracellularly. The relative ratio of the compound **10** and released Dox was determined with HPLC analysis with detection at 490 nm and at a specific time intervals after cellular lysis.

The cellular hydrolysis analysis showed that compound **10** was hydrolyzed intracellularly and released Dox in a time-dependent manner. Intracellular hydrolysis of compound **10** is faster when compared to hydrolysis in the serum within the same period. More than 75% of compound **10** was hydrolyzed intracellularly within 12 h (Figure 9) when compared to only

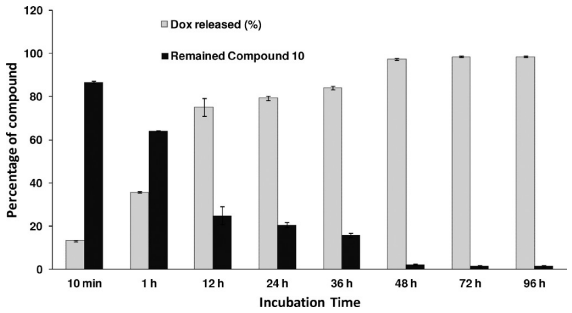

Figure 9. Cellular stability of compound **10**.

20% hydrolysis in the presence of the serum during the same period (Figure 8a). Approximately 98% of compound **10** is hydrolyzed intracellularly within 48 h (Figure 9), while only 30% of the compound is hydrolyzed in serum (Figure 8a). The intracellular hydrolysis pattern of compound **10** indicates that the antiproliferative activity of compound **10** is mainly due to sustained intracellular release of Dox. Thus, both cellular uptake and intracellular hydrolysis of lipophilic compound **10** contribute to sustained activity.

CONCLUSIONS

Fatty acyl derivatives of Dox succinate were synthesized by coupling of 14-hydroxyl group of Dox with the succinic anhydride followed by reaction with fatty amines or tetradecanol. In general, the fatty acyl derivatives exhibited higher antiproliferative activities in leukemia and colon cancer cells than breast and ovarian cell lines. The antiproliferative activity was retained through the conjugation of succinyl or fatty acyl to Dox. This approach is advantageous in various aspects. First, the compounds were found to be more lipophilic when compared to Dox. Second, *N*-tetradecyl amide derivative **10** exhibited a consistently higher antiproliferative activity among all of the derivatives and showed comparable activity with Dox. Third, compound **10** demonstrated rapid and higher cellular uptake than that of Dox in SK-OV-3 cells. Fourth, while Dox effluxed from the cells after 1 h, compound **10** showed prolonged retention and high cellular distribution with slow nuclear relocalization under a similar condition. The Topo II assay showed that compound **10** exhibited approximately 3−4-fold less topoisomerase inhibitory activity than Dox. Fifth, cellular studies showed that compound **10** was mainly hydrolyzed intracellularly and released Dox. The sustained intracellular hydrolysis and relocalizaton can allow a prolonged exposure of the tumor cells to Dox. Compound **10** with improved cellular uptake and retention versus Dox appears to be a promising Dox derivative for improving the anticancer profile of Dox. These data provide insights for designing additional Dox derivatives with optimal lipophilicity, retention, and sustained anticancer effects.

EXPERIMENTAL SECTION

Materials and Methods. Dox, HBTU, anhydrous dichloromethane (DCM), and other chemicals and reagents were purchased from Sigma-Aldrich Chemical Co. (Milwaukee, WI). HBTU in DCM was used as a coupling reagent. The chemical structures of final products were characterized by nuclear magnetic resonance spectra (^{1}H NMR, ^{13}C NMR) determined on a Varian NMR spectrometer (500 MHz). ^{13}C NMR spectra were fully decoupled. Chemical shifts were reported in parts per millions (ppm) using deuterated solvent peak or tetramethylsilane (internal) as the internal standards. The chemical structures of final products were confirmed by a high-resolution Biosystems QStar Elite time-of-flight electrospray mass spectrometer. Details of procedures and spectroscopic data of the respective compounds are presented below. Final compounds were purified on a Phenomenex Prodigy 10 μm ODS reversed-phase column (2.1 cm × 25 cm) with a Hitachi HPLC system using a gradient system of acetonitrile (CH_3CN) or methanol and water (CH_3OH/H_2O) (0−100%, pH 7.0, 60 min). The purity of final products (≥95%) was confirmed by analytical HPLC. The analytical HPLC was performed on a Hitachi analytical HPLC system using a C18 Shimadzu Premier 3 μm column (150 cm × 4.6 mm) and a gradient system (water/CH_3CN) and a flow rate of 1 mL/min with detection at 490 nm.

General Synthesis. All final compounds were synthesized using a similar procedure. *N*-Fmoc-doxorubicin hemisuccinate (**2**) was synthesized according to the previously reported procedure.[24] In brief, Dox was reacted with Fmoc-OSu to protect the free amino (NH_2) group, followed by reaction with succinic anhydride to afford **2**. Fatty acyl derivatives of Dox (**8**−**12**) were synthesized by a coupling reaction of **2** and the fatty amines or tetradecanol (in case of **12**) in the presence of HBTU followed by deprotection of Fmoc by piperidine. As a representative example, the synthesis of 14-doxorubicinyl succinyl *N*-tetradecylamide (**10**) derivative is described here. Compound **2** (86 mg, 0.1 mmol) was dissolved in dry DCM (10 mL). 1-Tetradecylamine (21 mg, 0.1 mmol) and HBTU (115 mg, 0.30 mmol) in dry DCM (20 mL) were added slowly to the reaction mixture. Next, DIPEA (50 mg, 0.39 mmol) was added to the mixture at room temperature. The solution was stirred for 3 h under nitrogen atmosphere. After completion of the reaction (monitored by analytical HPLC), water (50 mL) was added to the mixture, and the crude product was extracted with DCM (3 × 40 mL). The solvent was evaporated under reduced pressure, and piperidine solution in DMF (5%, 10 mL) was added to the residue. The reaction mixture turned to a dark blue color and was stirred for 10 min. The reaction was quenched by neutralization with acetic acid/trifluoroacetic acid. The red color was restored in the reaction mixture. The solvent was removed under reduced pressure. Water (50 mL) was added to the residue, and the solution was extracted with DCM (3 × 30 mL). After removal of DCM under reduced pressure, the crude product was purified by column chromatography over silica gel using DCM/methanol (0−20%) as the eluents to afford **10** (36 mg, 42.8%). The product was further purified on a reverse phase HPLC using a C18 column and methanol/water as a gradient mobile phase as described above.

14-[(*N*-Decylamido)succinyl]doxorubicin (8). Red solid (28 mg, 40.8% yield). IR (cm^{-1}, ATR): 2925, 1718 (C═O), 1641 (C═O str, amide), 1618, 1573, 1406, 1286, 1202, 1116, 1010, 986. UV/vis λ (nm): 496, 479, 289, 249, 229. ^{1}H NMR (500 MHz, CD_3OD, δ ppm): 7.90 (d, J = 7.4 Hz, 1H, ArC_1H), 7.81 (t, J = 8.0 Hz, 1H, ArC_2H), 7.54 (d, J = 8.5 Hz, 1H, ArC_3H), 5.44 (br s, 1H, H-1′), 5.31 (d, J_{gem} = 17.9 Hz, 1H, H-14), 5.10 (d, J_{gem} = 17.9 Hz, H-14), 5.05 (s, 1H, H-7), 4.31 (q, J = 6.4 Hz, 1H, H-5′), 4.01 (s, 3H, OCH_3), 3.67−3.65 (br s, 1H, H-4′), 3.58−3.52 (m, 1H, H-3′), 3.16 (t, J = 7.3 Hz, 2H, CH_2COO), 3.06 (d, J_{gem} = 18.8 Hz, 1H, H-10), 2.86 (d, J_{gem} = 18.8 Hz, 1H, H-10), 2.75

dx.doi.org/10.1021/jm201653u | J. Med. Chem. 2012, 55, 1500−1510

(t, J = 7.3 Hz, 2H, CH_2CONH), 2.53 (t, J = 6.9 Hz, 2H, CONHCH_2), 2.44 (d, 1H, J = 11.9 Hz, H-8), 2.12−2.06 (br d, 1H, H-8), 2.06−2.01 (m, 1H, H-2′), 1.90−1.85 (m, 1H, H-2′),1.49 (q, J = 6.1 Hz, 2H, CONHCH$_2$CH_2), 1.35−1.22 (m, 17H, methylene envelope, 7 × CH$_2$ and 6′-CH_3), 0.87 (t, J = 6.8 Hz, 3H, CH_3). ^{13}C NMR (125 MHz, CD$_3$OD, δ ppm): 208.77 (C$_{13}$═O), 188.35 (C$_{12}$═O), 188.02 (C$_5$═O), 174.13 (COOR), 173.91 (NH-C═O), 162.66 (C4), 157.51 (C6), 156.34 (C11), 137.47 (C2), 136.53 (C6a), 135.71 (C12a), 135.32 (C10a), 121.67 (C4a), 120.70 (C1), 120.57 (C3), 112.61 (C11a), 112.37 (C5a), 101.34 (C1′), 77.49 (C9), 71.76 (C7), 68.09 (C4′, C5′), 67.14 (C14), 57.29 (OCH$_3$), 40.66 (C3′), 37.38 (CH$_2$NHCO), 33.23 (C8), 31.66 (C10), 30.89, 30.88, 30.63, 30.63, 30.56, 30.38, 29.62 (methylene carbons), 28.18 (C2′), 23.88, 17.12 (5′-CH$_3$), 14.59 (CH$_3$). HR-MS (ESI-TOF): calcd for $C_{41}H_{54}N_2O_{13}$, 782.3626; found, 783.2648 [M + 1]$^+$.

14-[(*N*-Dodecylamido)succinyl]doxorubicin (9). Red solid (32 mg, 43.5% yield). IR (cm^{-1}, ATR): 3588, 2926, 1716 (C═O), 1642 (C═O str, amide), 1618, 1407, 1285, 1203, 1114, 1069, 1011, 986, 800, 723. UV/vis λ (nm): 478, 290, 254, 234. ^{1}H NMR (500 MHz, CD$_3$OD, δ ppm): 7.92 (d, J = 7.4 Hz, 1H, ArC$_1$H), 7.83 (t, J = 8.0 Hz, 1H, ArC$_2$H), 7.56 (d, J = 8.5 Hz, 1H, ArC$_3$H), 5.46 (br s, 1H, H-1′), 5.31 (d, J_{gem} = 17.9 Hz, 1H, H-14), 5.12 (d, J_{gem} = 17.9 Hz, H-14), 5.10−5.05 (br s, 1H, H-7), 4.32 (q, J = 6.4 Hz, 1H, H-5′), 4.03 (s, 3H, OCH$_3$), 3.67−3.65 (m, 1H, H-4′), 3.60−3.53 (m, 1H, H-3′), 3.17 (t, J = 7.3 Hz, 2H, CH$_2$COO), 3.12−3.06 (m, 1H, H-10), 2.92−2.83 (m, 1H, H-10), 2.72 (t, J = 7.3 Hz, 2H, CH$_2$CONH), 2.56 (t, J = 6.9 Hz, 2H, CONHCH$_2$), 2.47 (d, 2H, J = 14.7 Hz, H-8), 2.15−2.08 (br d, 1H, H-8), 2.07−2.03 (m, 1H, H-2′), 1.93−1.85 (m, 1H, H-2′), 1.52 (q, J = 6.1 Hz, 2H, CONHCH$_2$CH$_2$), 1.35−1.22 (m, 21H, methylene envelope, 9 × CH$_2$ and 6′-CH$_3$), 0.90 (t, J = 6.8 Hz, 3H, CH$_3$). ^{13}C NMR (100 MHz, CD$_3$OD, δ ppm): 206.81 (C$_{13}$═O), 186.46 (C$_{12}$═O), 186.10 (C$_5$═O), 172.15 (COOR), 171.90 (NH-C═O), 160.69 (C4), 155.57 (C6), 154.40 (C11), 137.04 (C2), 135.50 (C6a), 134.59 (C12a), 133.76 (C10a), 119.69 (C4a), 118.72 (C1), 118.55 (C3), 110.39 (C11a, C5a), 99.39 (C1′), 75.47 (C9), 69.83 (C7), 66.05 (C4′, C5′), 65.15 (C14), 55.28 (OCH$_3$), 44.18 (C3′), 38.69 (CH$_2$NHCO), 35.41 (C8), 31.28 (C10), 29.61, 28.93, 28.68, 28.58, 28.34, 27.64 (methylene carbons), 26.20 (C2′), 21.93 (CH$_2$CH$_3$), 15.13 (5′-CH$_3$), 12.63 (CH$_3$). HR-MS (ESI-TOF): calcd for $C_{43}H_{58}N_2O_{13}$, 810.3939; found, 811.3256 [M + 1]$^+$.

14-[(*N*-Tetradecylamido)succinyl]doxorubicin (10). Red solid (36 mg, 42% yield). IR (cm^{-1}, ATR): 3588, 3567, 3547, 2925, 1717 (C═O), 1641 (C═O str, amide), 1618, 1406, 1286, 1202, 1116, 1010, 986, 800, 722. UV/vis λ (nm): 494, 477, 288, 250, 229. ^{1}H NMR (500 MHz, CD$_3$OD, δ ppm): 7.89 (s, 1H, ArC$_1$H), 7.81 (t, 1H, J = 7.3 Hz, ArC$_2$H), 7.54 (d, 1H, J = 7.4 Hz, ArC$_3$H), 5.44 (s, 1H, H-1′), 5.31 (d, J_{gem} = 20.0 Hz, 1H, H-14), 5.10 (d, J_{gem} = 20 Hz, H-14), 5.09 (s, 1H, H-7), 4.31 (q, 1H, J = 5.0 Hz, H-5′), 4.01 (s, 3H, OCH$_3$), 3.67−3.65 (br s, 1H, H-4′), 3.59−3.55 (m, 1H, H-3′), 3.19−3.15 (m, 2H, CH$_2$COO), 3.06 (d, J_{gem} = 15.0 Hz, 1H, H-10), 3.00 (d, J_{gem} = 15.0 Hz, 1H, H-10), 2.75 (t, J = 5.0 Hz, 2H, CH$_2$CONH), 2.54 (t, J = 5.0 Hz, 2H, CONHCH$_2$), 2.50−2.43 (m, 2H, H-8), 2.10−2.01 (m, 1H, H-2′), 1.92−1.85 (m, 1H, H-2′), 1.49 (q, 2H, J = 7.0 Hz, CONHCH$_2$CH$_2$), 1.35−1.22 (m, 25H, methylene envelope, 11 x CH$_2$ and 6′-CH$_3$), 0.89 (t, J = 6.7 Hz, 3H, CH$_3$). ^{13}C NMR (125 MHz, CD$_3$OD, δ ppm): 207.21 (C$_{13}$═O), 186.70 (C$_{12}$═O), 186.37 (C$_5$═O), 172.56 (COOR), 172.31 (NH-C═O), 161.05 (C4), 155.93 (C6), 154.74 (C11), 135.88 (C2), 134.91 (C6a), 134.11 (C12a), 133.74 (C10a), 120.02 (C4a), 119.11 (C1), 118.97 (C3), 110.98 (C11a), 110.75 (C5a), 99.80 (C1′), 75.88 (C9), 70.15 (C7), 66.51 (C4′, C5′), 65.61 (C14), 55.70 (OCH$_3$), 39.12 (C3′), 35.72 (NHCOCH$_2$), 31.92 (C8), 31.67 (C10), 30.07, 29.43, 29.41, 29.39, 29.35, 29.28, 29.10, 29.09, 29.07, 29.01, 28.79, 28.05, 26.62 (methylene carbons), 26.55 (C2′), 22.33 (CH$_2$CH$_3$), 15.56 (5′-CH$_3$), 13.05 (CH$_3$). HR-MS (ESI-TOF): calcd for $C_{45}H_{62}N_2O_{13}$, 838.4252; found, 839.3789 [M + 1]$^+$.

14-[(*N*-Hexadecylamido)succinyl]doxorubicin (11). Red solid (38 mg, 41.4% yield). IR (cm^{-1}, ATR): 3588, 2926, 1716 (C═O), 1642 (C═O str, amide), 1618, 1407, 1285, 1203, 1114, 1069, 1011, 986, 800, 723. UV/vis λ (nm): 494, 477, 289, 249, 229. ^{1}H NMR (500 MHz, DMSO-d_6, δ ppm): 8.10 (s, 1H, ArC$_1$H), 8.01 (s, 1H, ArC$_2$H), 7.84 (s, 1H, ArC$_3$H), 5.86 (s, 1H, OH), 5.63 (s, 1H, OH), 5.46 (br s, 1H, H-1′), 5.40 (d, J_{gem} = 17.9 Hz, 1H, H-14), 5.35 (d, J_{gem} = 17.9 Hz, H-14), 5.11−5.15 (br s, 1H, H-7), 4.40 (q, 1H, J = 5.0 Hz, H-5′), 4.17 (s, 3H, OCH$_3$), 3.77−3.72 (m, 1H, H-4′), 3.69−3.67 (m, 1H, H-3′), 3.18−3.15 (m, 2H, CH$_2$COO), 3.09−3.06 (m, 1H, H-10), 2.78−2.74 (m, 1H, H-10), 2.69−2.65 (m, 2H, CH$_2$CONH), 2.59−2.50 (m, 2H, CONHCH$_2$), 2.49−2.30 (m, 2H, H-8), 1.90−1.80 (m, 1H, H-2′), 1.75−1.60 (m, 1H, H-2′), 1.53 (q, 2H, J = 7.0 Hz, CONHCH$_2$CH$_2$), 1.50−1.35 (m, 29H, methylene envelope, 13 x CH$_2$ and 6′-CH$_3$),1.05−1.01 (m, 3H, CH$_3$). ^{13}C NMR (125 MHz, DMSO-d_6, δ ppm): 207.80 (C$_{13}$═O), 186.63 (C$_{12}$═O), 186.53 (C$_5$═O), 171.92 (COOR), 170.18 (NH-C═O), 160.85 (C4), 155.96 (C6), 154.48 (C11), 136.33 (C2), 135.12 (C6a), 134.76 (C12a), 133.90 (C10a), 120.01 (C4a), 119.82 (C1), 119.05 (C3), 110.80 (C11a), 110.71 (C5a), 99.25 (C1′), 75.06 (C9), 69.78 (C7), 69.62 (C5′), 66.14 (C4′), 65.53 (C14), 56.64 (OCH$_3$), 46.60 (C3′), 38.52 (CH$_2$NHCO), 38.42 (CH$_2$COOR), 36.09 (NHCOCH$_2$), 33.66 (C8), 31.85 (C10), 31.29, 29.84, 29.82, 29.05, 29.03, 29.00, 28.86, 28.77, 28.74, 28.70, 24.49 (methylene carbons), 26.39 (C2′), 22.15, 22.09, 21.65, 16.63 (5′-CH$_3$), 13.95 (CH$_3$). HR-MS (ESI-TOF): calcd for $C_{47}H_{66}N_2O_{13}$, 866.4565; found, 867.3724 [M + 1]$^+$.

14-[(Tetradecanoyl)succinyl]doxorubicin (12). This product was obtained by the reaction of *N*-Fmoc Dox hemisuccinate (**2**, 86 mg, 0.1 mmol) with tetradecanol (23 mg, 0.11 mmol) by following a similar procedure described above for compound **10**. Red brown solid (34 mg, 40.8% yield). IR (cm^{-1}, ATR): 3346, 2923, 2848, 1719 (C═O), 1614, 1575, 1445, 1407, 1280, 1205, 1017, 980. UV/vis λ (nm): 494, 477, 289, 249, 229. ^{1}H NMR (500 MHz, CD$_3$OD, δ ppm): 7.89 (t, J = 5.0 Hz, 1H, ArC$_1$H), 7.79 (s, 1H, ArC$_2$H), 7.71 (t, 1H, J = 7.3 Hz), 7.44 (d, 1H, J = 7.4 Hz, ArC$_3$H), 5.34 (br s, 1H, H-1′), 5.24 (d, J_{gem} = 20.0 Hz, 1H, H-14), 5.02 (d, J_{gem} = 20.0 Hz, H-14), 4.94 (s, 1H, H-7), 4.21 (q, 1H, J = 5.0 Hz, H-5′), 3.91 (s, 3H, OCH$_3$), 3.56 (br s, 1H, H-4′), 3.48−3.45 (m, 1H, H-3′), 3.08−3.05 (m, 1H, H-10), 2.96−2.88 (m, 1H, H-10), 2.65 (t, J = 5.0 Hz, 2H, CH$_2$COO), 2.58 (t, 2H, J = 5.4 Hz, COOCH$_2$), 2.44 (t, J = 5 Hz, 2H, CH$_2$COO), 2.40−2.32 (m, 1H, H-8), 2.00−1.92 (m, 1H, H-8), 1.80−1.77 (m, 1H, H-2′), 1.53−1.49 (m, 1H, H-2′), 1.39 (q, 2H, J = 7.0 Hz, COOCH$_2$CH$_2$), 1.25−1.10 (m, 25H, methylene envelope, 11 × CH$_2$ and 6′-CH$_3$), 0.80 (t, J = 6.65 Hz, 3H, CH$_3$). ^{13}C NMR (125 MHz, CD$_3$OD, δ ppm): 207.39 (C$_{13}$═O), 188.57 (C$_{12}$═O), 188.10 (C$_5$═O), 174.20 (O-C═O), 172.01 (O-C═O), 160.19 (C4), 156.45 (C6), 151.81 (C11), 136.27 (C2), 135.23 (C6a), 135.19 (C12a), 133.78 (C10a), 120.72 (C4a), 120.53 (C1), 119.48 (C3), 108.87 (C11a), 101.35 (C1′), 77.50 (C9), 71.83 (C7), 68.12 (C4′), 68.02 (C5′), 63.15 (C14), 57.28 (OCH$_3$), 39.75 (C3′), 37.12 (CH$_2$COO), 33.82 (C8), 33.24 (C10), 31.00, 30.96, 30.94, 30.92, 30.87, 30.77, 30.67, 30.64, 29.86, 27.19 (methylene carbons), 27.11 (C2′), 23.90 (CH$_2$CH$_3$), 17.12 (5′-CH$_3$), 14.60 (CH$_3$). HR-MS (ESI-TOF): calcd for $C_{45}H_{61}NO_{14}$, 839.4092; found, 840.3509 [M + 1]$^+$.

14-Doxorubicinyl Succinate Ester (13). This product was obtained by the deprotection reaction of *N*-Fmoc Dox hemisuccinate (**2**, 43 mg, 0.05 mmol) with piperidine in DMF (8%, 5 mL). The reaction mixture was neutralized with acetic acid, and the solvent was evaporated under vacuum. The product was purified on HPLC using methanol/water gradient system. Red solid (30 mg, 39.8% yield). IR (cm^{-1}, ATR): 3346, 2923, 2848, 1719 (C═O), 1614, 1575, 1445, 1407, 1280, 1205, 1017, 980. UV/vis λ (nm): 494, 477, 289, 249, 229. ^{1}H NMR (500 MHz, CD$_3$OD + CDCl$_3$, δ ppm): 13.99 (s, 1H, PhOH), 13.27 (s, 1H, COOH), 7.99 (d, J = 7.5 Hz, 1H, ArC$_1$H), 7.85 (t, 1H, J = 8.3 Hz, ArC$_2$H), 7.73 (s, 1H, OH), 7.54 (d, 1H, J = 8.4 Hz, ArC$_3$H), 5.49 (d, 1H, J = 8.4 Hz, H-1′), 5.33 (d, J_{gem} = 17.9 Hz, 1H, H-14), 5.11 (d, J_{gem} = 17.9 Hz, H-14), 5.11 (s. 1H, H-7), 4.82 (s, 1H, OH), 4.74 (s,1H, OH), 4.29 (q, J = 7.3 Hz, 1H, H-5′), 4.06 (s, 3H, OCH$_3$), 3.67 (br s, 1H, H-4′), 3.55−3.52 (m, 1H, H-3′), 3.17−3.13 (m, 2H, H-10), 2.77 (t, 2H, J = 7.0 Hz, CH$_2$COOH), 2.59 (t, 2H, J = 6.9 Hz, CH$_2$COOR), 2.44 (d, 1H, J = 14.4 Hz, H-8), 2.14−2.01 (m, 2H, H-8 and H-2′), 1.89 (dd, 1H, J = 13.3 Hz, J = 5.1 Hz, H-2′), 1.31 (d, 3H, J = 6.5 Hz, 6′-CH$_3$). ^{13}C NMR (125 MHz, CD$_3$OD + CDCl$_3$, δ ppm): 208.71 (C$_{13}$═O), 188.26 (C$_{12}$═O), 187.87 (C$_5$═O), 176.85 (COOH), 173.84 (O-C═O), 162.46 (C4), 157.36 (C6), 156.21 (C11), 137.36 (C2), 136.38 (C6a), 135.45 (C12a), 135.19 (C10a),

dx.doi.org/10.1021/jm201653u | J. Med. Chem. 2012, 55, 1500−1510

121.53 (C4a), 120.67 (C1), 120.40 (C3), 112.49 (C11a), 112.62 (C5a), 101.10 (C1′), 77.38 (C9), 71.48 (C7), 67.95 (C5′), 67.89 (C4′), 67.05 (C14), 57.28 (OCH_3), 37.15 (C3′), 33.44 (C8), 30.84 (C10), 30.00 (CH_2COO), 29.43 (C2′), 10.04 (5′-CH_3). HR-MS (ESI-TOF): calcd for $C_{31}H_{33}NO_{14}$, 643.1901; found, 644.1076 $[M + 1]^+$.

Determination of Partition Coefficient. Partition coefficients of Dox derivatives were determined using *n*-octanol/water distribution shake flask method. In a typical method, 100 μg of the Dox derivative was partitioned between 200 μL of 1-octanol and 200 μL of distilled water. The mixture was shaken for 3 h, and the organic and aqueous phases were allowed to separate. The concentration of the Dox derivatives was measured in both phases using UV spectroscopy by comparing with a standard solution UV spectrum. The experiment was repeated three times, and an average of the readings was taken. The partition coefficient (*P*) of the sample was then determined by the following equation, *P* = concentration of sample in *n*-octanol/concentration of sample in water. The reported Log *P* is the average of three readings ± standard deviations for all derivatives.

Topo II Decatenation Assay. The topoisomearase II assay kit (catalog no. 1001-1 was purchased from TopoGEN, Inc. (Port Orange, FL). Eukaryotic Topo II was assayed by decatenation of kDNA and monitoring the appearance of a smaller DNA (decatenated DNA circles). Reaction mixtures containing kDNA (0.1 μg) in a final volume of 20 μL and 1X reaction buffer containing Tris-HCl (50 mM, pH 8.0), NaCl (150 mM), $MgCl_2$ (10 mM), dithiothreitol (0.5 mM), and ATP (2 mM) were incubated for 30 min at 37 °C without and with Dox, **14**, and **10** at 1, 5, 10, 15, 20, and 25 μM final concentration. Reactions were terminated with the addition of 0.4 volume of stop buffer (5% sarkosyl, 0.125% bromophenol blue, and 25% glycerol). One unit of Topo II is defined as the amount of enzyme required to fully decatenate 0.1 μg of kDNA in 30 min at 37 °C. The decatenation products were analyzed on 1% agarose gels having 0.5 μg ethidium bromide/mL. Eukaryotic Topo II products were separated at 108 V, which allowed rapid resolution of catenated networks from the minicircles. Gels were photographed by ethidium bromide fluorescence on Typhoon Imager.

Cell Culture. Human leukemia cell line CCRF-CEM (ATCC no. CCL-119), breast adenocarcinoma MDA-MB-468 (ATCC no. HTB-132), breast adenocarcinoma MDA-MB-361 (ATCC no. HTB-27), ovarian adenocarcinoma SK-OV-3 (ATCC no. HTB-77), and colon adenocarcinoma HT-29 (ATCC no. HTB-38) were obtained from American Type Culture Collection. The cells were grown on 75 cm^2 cell culture flasks with RPMI-16 medium for leukemia and EMEM medium for other cell lines and supplemented with 10% FBS and 1% penicillin−streptomycin solution (10000 units of penicillin and 10 mg of streptomycin in 0.9% NaCl) in a humidified atmosphere of 5% CO_2, 95% air at 37 °C.

Cell Proliferation Assay. The cell proliferation assay of synthesized Dox derivatives (**8**−**12**) was evaluated in MDA-MB-361, MDA-MB-468, CCRF-CEM, SK-OV-3, and HT-29 cells and was compared with that of Dox. The cell proliferation assay was carried out using CellTiter 96 aqueous one solution cell proliferation assay kit (Promega). As a representative example, CCRF-CEM cells were suspended in 5×10^5/mL, and 100 μL of the cell suspension was placed in each well of the 96-well culture plate. The cells were incubated with Dox and its derivatives (**8**−**12**, 1 μM) in 4% DMSO and tested in triplicate. Incubation was carried out at 37 °C in an incubator supplied with 5% CO_2 for 24−120 h. At the end of the sample exposure period (24−120 h), 20 μL of CellTiter 96 aqueous solution was added. The plate was returned to the incubator for 1 h in a humidified atmosphere at 37 °C. The absorbance of the formazan product was measured at 490 nm using a microplate reader. The percentage of cell survival was calculated as OD value of cells treated with the test compound − OD value of culture medium/(OD value of control cells − OD value of culture medium) × 100%.

Cell Cytotoxicity Assay. The cytotoxicity of Dox and compound **10** was determined against ovarian carcinoma cells SK-OV-3 by MTT assay. All cells were plated overnight in 96-well plates with a density of 5000 cells per well in 0.1 mL of appropriate growth medium at 37 °C. Different concentrations of Dox or compound **10** (up to a maximum of 10 μM) were incubated with the cells for 2 h. Dox or compound **10** was removed from media by replacing with fresh media, and the cells were kept in an incubator for another 72 h. The cells without compounds were included in each experiment as controls. After 72 h of incubation, 20 μL of MTT was added, and incubation was continued for 2 h. The absorbance of the formazan product was measured at 490 nm using a microplate reader. The percentage of cytotoxicity was calculated as (OD value of untreated cells − OD value of treated cells)/OD value of untreated cells × 100%.

Confocal Microscopy. Ovarian carcinoma cells (SK-OV-3) were seeded with EMEM media overnight on coverslips in six-well plates. Then, the medium was removed and washed with opti-MEM. The cells were treated with Dox or Dox conjugate (5 μM) in opti-MEM for 1 h at 37 °C. After 1 h of incubation, the media containing the compound were removed followed by washing with PBS three times. Then, coverslips were placed on a drop of mounting media on a microscope slide with cells-attached side facing down. Laser scanning confocal microscopy was carried out using Carl Zeiss LSM 510 system. The cells were imaged using rhodamine and phase contrast channels. In the case of drug efflux studies, after the 1 h incubation period, the medium containing drugs was removed and washed with opti-MEM. Then, fresh medium with serum was added into the cells. After 24 h, the medium was removed and washed with PBS three times, and then, the cells were visualized under confocal microscopy.

FACS Analysis. Ovarian carcinoma cells were plated overnight in six-well plates (2×10^5 cells/well) in EMEM media. Then, Dox (5 μM) and compound **10** (5 μM) were added in opti-MEM to the cells. The plates were incubated for 30 min at 37 °C. After 30 min of incubation, the media containing drugs were removed. The cells were digested with 0.25% trypsin/0.53 mM EDTA for 5 min to detach from the plate. Then, the cells were centrifuged and washed twice with PBS. Finally, the cells were resuspended in flow cytometry buffer and analyzed by flow cytometry (FACSCalibur: Becton Dickinson) using FL2 channel and CellQuest software. The data presented are based on the mean fluorescence signal for 10000 cells collected. All assays were performed in triplicate.

Stability Studies. The stability of compound **10** was evaluated in FBS and PBS. FBS was obtained from ATCC (Manassas, VA). PBS was purchased from Invitrogen and used as supplied. Compound **10** (50 μL of 1 mM solution in DMSO) was incubated in FBS (1 mL, 100%) or PBS (1 mL, pH 7.0) at 37 °C with intermediate shaking. About 30 μL of the reaction solution was removed at different time intervals (starting from 10 min to 96 h), diluted with an equal amount of water, and analyzed by analytical HPLC with detection at 490 nm. The area under the curve was used to calculate the percentage of released Dox and remaining compound **10** at a given time. The relative percentage of Dox and compound **10** was plotted on a graph to obtain the stability in FBS and PBS at the particular time intervals of incubation.

Cellular Hydrolysis. Intracellular hydrolysis of compound **10** and accumulation of Dox and compound **10** were determined in CCRF-CEM cells by HPLC analysis. CCRF-CEM cells were grown in 75 cm^2 culture flasks with serum-free RPMI medium to ∼70−80% confluence (1.37×10^7 cells/mL). The medium was replaced with fresh RPMI medium having compound **10** (1 μM), and the cells were incubated at 37 °C for 4 h. The medium containing compound **10** was carefully removed by using centrifugation and replaced with fresh RPMI serum-free medium. The cells were partitioned/transferred to culture plates (six-well) having 1.37×10^7 cells per well in 5 mL of medium and incubated for the indicated time. After incubation, the cells were collected by centrifugation. The medium was removed carefully by decantation, and cell pallets were washed with ice-cold PBS to remove any medium. The cell pallets were thoroughly extracted with an equal volume of methanol, chloroform, and isopropanol mixture (4:3:1 v/v/v) and filtered through 0.2 μm filters. The relative Dox and compound **10** concentrations in cell lysates were quantified by analytical HPLC analysis at 490 nm using the water/acetonitrile solvent method as described above. The relative Dox and compound **10** percent concentrations were given by standard graph with an average of three experiments and deviation reflected by the standard deviation.

■ ASSOCIATED CONTENT

Supporting Information

^{1}H NMR, ^{13}C NMR, DEPT, HSQC, COSY, UV−visible spectra, IR spectra, analytical HPLC, and PBS and FBS stability analysis for representative compounds. This material is available free of charge via the Internet at http://pubs.acs.org.

■ AUTHOR INFORMATION

Corresponding Author

*Tel: +1-401-874-4471. Fax: +1-401-874-5787. E-mail: kparang@uri.edu.

Notes

The authors declare no competing financial interest.

■ ACKNOWLEDGMENTS

We acknowledge the financial support from the American Cancer Society Grant #RSG-07-290-01-CDD.

■ ABBREVIATIONS USED

DCM, dichloromethane; Dox, doxorubicin; FACS, fluorescence-activated cell sorter; FBS, fetal bovine serum; Fmoc-OSu, *N*-(9-fluorenylmethoxycarbonyloxy)succinimide; DIPEA, *N*,*N*-diisopropylethylamine; HBTU, 1,1,3,3-tetramethyluronium hexafluorophosphate; kDNA, kinetoplast DNA; Log *P*, partition coefficient; PgP, P-glycoprotein; PBS, phosphate-buffered saline solution; Topo II, topoisomerase II

■ REFERENCES

(1) Garattini, S. Pharmacokinetics in cancer chemotherapy. *Eur. J. Cancer* **2007**, *43*, 271−282.

(2) Takakura, Y.; Hashida, M. Macromolecular drug carrier systems in cancer chemotherapy: Macromolecular prodrugs. *Crit. Rev. Oncol/Hematol.* **1995**, *18*, 207−231.

(3) Mohanty, C.; Sahoo, S. K. The in vitro stability and in vivo pharmacokinetics of curcumin prepared as an aqueous nanoparticulate formulation. *Biomaterials* **2010**, *31*, 6597−6611.

(4) Vincenzi, B.; Frezza, A. M.; Santini, D.; Tonini, G. New therapies in soft tissue sarcoma. *Expert Opin. Emerging Drugs* **2010**, *15*, 237−248.

(5) Nori, A.; Kopecek, J. Intracellular targeting of polymer-bound drugs for cancer chemotherapy. *Adv. Drug Delivery Rev.* **2005**, *57*, 609−636.

(6) (a) Tang, Y.; McGoron, A. J. Combined effects of laser-ICG photothermotherapy and doxorubicin chemotherapy on ovarian cancer cells. *J. Photochem. Photobiol. B: Biol.* **2009**, *97*, 138−144. (b) Hu, F. Q.; Wu, X. L.; Du, Y. Z.; You, J.; Yuan, H. Cellular uptake and cytotoxicity of shell crosslinked stearic acid-grafted chitosan oligosaccharide micelles encapsulating doxorubicin. *Eur. J. Pharm. Biopharm.* **2008**, *69*, 117−125.

(7) Raoul, J. L.; Heresbach, D.; Bretagne, J. F.; Ferrer, D. B.; Duvauferrier, R.; Bourguet, P.; Messner, M.; Gosselin, M. Chemoembolization of hepatocellular carcinomas a study of the biodistribution and pharmacokinetics of doxorubicin. *Cancer* **1992**, *70*, 585−590.

(8) Rahman, A.; Carmichael, D.; Harris, M.; Roh, J. K. Comparative pharmacokinetics of free doxorubicin and doxirubicin entrapped in cardiolipin liposomes. *Cancer Res.* **1986**, *46*, 2295−2299.

(9) Tang, X. H.; Xie, P.; Ding, Y.; Chu, L. Y.; Hou, J. P.; Yang, J. L.; Song, X.; Xie, Y. M. Synthesis, characterization, and in vitro and in vivo evaluation of a novel pectin-adriamycin conjugate. *Bioorg. Med. Chem.* **2010**, *18*, 1599−1609.

(10) Riganti, C.; Voena, C.; Kopecka, J.; Corsetto, P. A.; Montorfano, G.; Enrico, E.; Costamagna, C.; Rizzo, A. M.; Ghigo, D.; Bosia, A. Liposome-encapsulated doxorubicin reverses drug resistance by inhibiting P-glycoprotein in human cancer cells. *Mol. Pharmaceutics* **2011**, *8*, 683−700.

(11) Takemura, G.; Fujiwara, H. Doxorubicin-induced cardiomyopathy from the cardiotoxic mechanisms to management. *Prog. Cardiovasc. Dis.* **2007**, *49*, 330−352.

(12) Ayla, S.; Seckin, I.; Tanriverdi, G.; Cengiz, M.; Eser, M.; Soner, B. C.; Oktem, G. Doxorubicin induced nephrotoxicity: Protective effect of nicotinamide. *Int. J. Cell Biol.* **2011**, 390238. Epub **2011** Jun 16

(13) Elsadek, B.; Graeser, R.; Wamecke, A.; Unger, C.; Saleem, T.; El-Melegy, N. Optimization of an albumin-binding prodrug of doxorubicin that is cleaved by prostate-specific antigen. *ACS Med. Chem. Lett.* **2010**, *1*, 234−238.

(14) Chaudhuri, P.; Paraskar, A.; Soni, S.; Mashelkar, R. A.; Sengupta, S. Fullerenol-cytotoxic conjugates for cancer chemotherapy. *ACS Nano* **2009**, *3*, 2505−2514.

(15) Dhar, S.; Reddy, E. M.; Shiras, A.; Pokharkar, V.; Prasad, B. L. Natural gum reduced/stabilized gold nanoparticles for drug delivery formulations. *Chemistry* **2008**, *14*, 10244−10250.

(16) Kumar, S. A.; Peter, Y. A.; Nadeau, J. L. Facile biosynthesis, separation and conjugation of gold nanoparticles to doxorubicin. *Nanotechnology* **2008**, *19*, 495101.

(17) You, J.; Zhang, G.; Li, C. Exceptioanlly high payload of doxorubicin in hollow gold nanosphere for near-infrared light-triggered drug release. *ACS Nano* **2010**, *4*, 1033−1041.

(18) Alba, E.; Ruiz-Borrego, M.; Margeli, M.; Rodriguez-Lescure, A.; Sanchez-Rovira, P.; Ruiz, A.; Mel-Lorenzo, J. R.; Ramos-Vazquez, M.; Ribelles, N.; Calvo, E.; Casado, A.; Marquez, A.; Vicente, D.; Garcia-Saenz, J. A.; Martin, M. Maintenance treatment with pegylated liposomal doxorubicin versus observation following induction chemotherapy for metastatic breast cancer: GEICAM 2001−01 study. *Breast Cancer Res. Treat.* **2010**, *122*, 169−176.

(19) Rusetskaya, N. V.; Lukyanova, N. Y.; Chekhun, V. F. Molecular profile and cell cycle in MCF-7 and MCF-7/Dox cells exposed to conventional and liposomal forms of doxorubicin. *Exp. Oncol.* **2009**, *31*, 140−143.

(20) Huober, J.; Fett, W.; Nusch, A.; Neise, M.; Schmidt, M.; Wischnik, A.; Gerhardt, S.; Goehler, T.; Luck, H. J.; Rost, A. A multicentric observational trial of pegylated liposomal doxorubicin for metastatic breast cancer. *BMC Cancer* **2010**, *10*, 2.

(21) Stevens, P. J.; Lee, R. J. Formulation kit for liposomal doxorubicin composed of lyophilized liposomes. *Anticancer Res.* **2003**, *23*, 439−442.

(22) Abraham, S. A.; Waterhouse, D. N.; Mayer, L. D.; Cullis, P. R.; Madden, T. D.; Bally, M. B. The liposomal formulation of doxorubicin. *Methods Enzymol.* **2005**, *391*, 71−97.

(23) Meyer-Losic, F.; Quinonero, J.; Dubois, V.; Alluis, B.; Dechambre, M.; Michel, M.; Cailler, F.; Fernandez, A. M.; Trouet, A.; Kearsey, J. Improved therapeutic efficacy of doxorubicin through conjugation with a novel peptide drug delivery technology (Vectocell). *J. Med. Chem.* **2006**, *49*, 6908−6916.

(24) Ché, C.; Yang, G.; Thiot, C.; Lacoste, M.-C.; Currie, J.-C.; Demeule, M.; Régina, A.; Béliveau, R.; Castaigne, J.-P. New angiopep-modified doxorubicin (ANG1007) and etoposide (ANG1009) chemotherapeutics with increased brain penetration. *J. Med. Chem.* **2010**, *53*, 2814−2824.

(25) Zhu, S.; Hong, M.; Zhang, L.; Tang, G.; Jiang, Y.; Pei, Y. PEGylated PAMAM dendrimer-doxorubicin conjugates: In vitro evaluation and in vivo tumor accumulation. *Pharm. Res.* **2010**, *27*, 161−174.

(26) Varaprasad, K.; Ravindra, S.; Reddy, N. N.; Vimala, K.; Raju, K. M. Design and development of temperature sensitive porous poly(NIPAAm-AMPS) hydrogels for drug release of doxorubicin-a cancer chemotherapy drug. *J. Appl. Polym. Sci.* **2010**, *116*, 3593−3602.

(27) Ibsen, S.; Zahavy, E.; Wrasdilo, W.; Berns, M.; Chan, M.; Esener, S. A novel doxorubicin prodrug with controllable photolysis activation for cancer chemotherapy. *Pharm. Res.* **2010**, *27*, 1848−1860.

(28) Chhikara, B. S.; Parang, K. Development of cytarabine prodrugs and delivery systems for leukemia treatment. *Expert Opin. Drug Delivery* **2010**, *7*, 1399−1414.
(29) Wang, Y.; Li, L.; Jiang, W.; Yang, Z.; Zhang, Z. Synthesis and preliminary antitumor activity evaluation of a DHA and doxorubicin conjugate. *Bioorg. Med. Chem. Lett.* **2006**, *16*, 2974−2977.
(30) Kratz, F. DOXO-EMCH (INNO-206):The first albumin-binding prodrug of doxorubicin to enter clinical trials. *Expert Opin. Invest. Drugs* **2007**, *16*, 855−866.
(31) Chhikara, B. S.; St. Jean, N.; Mandal, D.; Kumar, A.; Parang, K. Fatty acyl amide derivatives of doxorubicin: Synthesis and in vitro anticancer activities. *Eur. J. Med. Chem.* **2011**, *46*, 2037−2042.
(32) Patel, D. J.; Kozlowski, S. A.; Rice, J. A. Hydrogen bonding, overlap geometry, and sequence specificity in anthracycline antitumor antibiotic.DNA complexes in solution. *Proc. Natl. Acad. Sci. U.S.A.* **1981**, *78*, 3333−3337.
(33) Quigley, G. J.; Wang, A. H.; Ughetto, G.; van der Marel, G.; van Boom, J. H.; Rich, A. Molecular structure of an anticancer drug-DNA complex: daunomycin plus d(CpGpTpApCpG). *Proc. Natl. Acad. Sci. U.S.A.* **1980**, *77*, 7204−7208.